A Completeness Analysis of the National Seismic Network of Italy

D. Schorlemmer

Southern California Earthquake Center, University of Southern California,

3651 Trousdale Parkway, MC-0740, Los Angeles, CA 90089-0740, USA

F. Mele

Istituto Nazionale di Geofisica e Vulcanologia, Via di Vigna Murata 605,

00143 Roma, Italy

W. Marzocchi

Istituto Nazionale di Geofisica e Vulcanologia, Via di Vigna Murata 605,

00143 Roma, Italy

D. Schorlemmer, Southern California Earthquake Center, University of Southern California, 3651 Trousdale Parkway, MC-0740, Los Angeles, CA 90089-0740, USA. (ds@usc.edu)

F. Mele, Istituto Nazionale di Geofisica e Vulcanologia, Via di Vigna Murata 605, 00143 Roma, Italy. (f.mele@ingv.it)

W. Marzocchi, Istituto Nazionale di Geofisica e Vulcanologia, Via di Vigna Murata 605, 00143 Roma, Italy. (warner.marzocchi@ingv.it)

Abstract. We present the first detailed study of earthquake detection capabilities of the Italian National Seismic Network and of the completeness threshold of its earthquake catalog. The network in its present form started operating on 16 April 2005 and is a significant improvement over the previous networks. For our analysis, we employed the PMC method as introduced by *Schorlemmer and Woessner* [2008]. This method does not estimate completeness from earthquakes samples as traditional methods, mostly based on the linearity of earthquake-size distributions. It derives detection capabilities for each station of the network and synthesizes them into maps of detection probabilities for earthquakes of a given magnitude. Thus, this method avoids the many assumptions about earthquake distributions that traditional methods make. The results show that the Italian National Seismic Network is complete at $M = 2.9$ for the entire territory excluding the islands of Sardinia, Pantelleria, and Lampedusa. At the $M = 2.5$ level, which is the reporting threshold level of the Italian Civil Protection, the network may miss events in southern parts of Apulia and the western part of Sicily. The stations are connected through many different telemetry links to the operational datacenter in Rome. Scenario computations show that no significant drop in completeness occurs if one of the three major links fail, indicating a well-balanced network setup.

Introduction

Earthquake catalogs are one of the most important products of seismological networks. Their completeness in detecting earthquakes down to small magnitudes is a crucial parameter to many studies in earthquake statistics, source seismology, and probabilistic seismic hazard analysis. Estimating completeness incorrectly may subsequently lead to wrong results when, e. g., determining seismic rate changes, investigating the development of aftershock sequences, or computing b-values of the Gutenberg-Richter distribution [*Gutenberg and Richter*, 1944; *Ishimoto and Iida*, 1939]. Such wrong results then propagate into, e. g., seismic hazard assessment. Almost any interpretation of seismic activity strongly depends on correct completeness estimates.

Completeness describes the magnitude of the smallest events that can be reliably and completely detected by the network. It is a function of space and time as networks change over time and their spatial coverage is not uniform. Five different methods for estimating network recording completeness exist, see [*Schorlemmer and Woessner*, 2008] for a more detailed description and discussion about available techniques: (1) Waveform-based techniques investigating signal-to-noise ratios at stations [*Gomberg*, 1991; *Kvaerna et al.*, 2002a, b; *Enescu et al.*, 2007, in print]. These results are combined with assumptions about wave propagation for estimating network completeness. (2) The method of *Rydelek and Sacks* [1989] derives completeness from the day-to-night activity ratio per magnitude bin of earthquake samples. This method makes the assumptions that the computed completeness is representative for the spatial extent and the period used for sampling the events. (3) Further methods based on earthquake samples exist that estimate the completeness magnitude, M_{c}, as the deviation point from the Gutenberg-Richter line (b-value fit) in the cumulative frequency-magnitude distribution [*Cao and Gao*, 2002; *Wiemer and Wyss*, 2000; *Marsan*, 2003; *Woessner and Wiemer*, 2005; *Amorèse*, 2007]. These methods additionally need to assume that earthquake populations exhibit a Gutenberg-Richter power law. All earthquake sample-based methods suffer from their inability to assess completeness in seismically inactive areas. (4) Earthquake samples are also used in the method developed by *Tinti and Mulargia* [1985]. It assumes that seismicity is a stationary Poissonian process and incompleteness is derived from deviation from stationarity. (5) *Schorlemmer and Woessner* [2008] developed a seismicity-based method that describes completeness in a probabilistic sense. It derives completeness values in space and time from station detection probabilities, which are derived from observed seismicity and reflect the characteristics of each station (e. g., station quality, site conditions, station coupling, noise level, etc.). This technique avoids the aforementioned assumptions and provides a full description of recording probabilities over space, time, and magnitude.

We present a comprehensive study of the recording completeness for the Italian *Rete Sismica Nazionale* (National Seismic Network, RSN), operated by the Istituto Nazionale di Geofisica e Vulcanologia (INGV). We focus on analyzing network recording probabilities for 1 January 2008. This includes mapping of completeness and recording probabilities for different magnitudes as well as investigations about the dependence of completeness on depth. To investigate the effects of network failures on completeness, we present different computations for the most likely failure scenarios.

The National Seismic Network

The Italian National Seismic Network has been strongly improved in the last 10 years. During this period, the number of earthquakes located within the coverage of the RSN doubled, and the minimum magnitude of completeness of the Italian Seismic Bulletin (as computed from the Gutenberg-Richter distribution) decreased from $M_c \approx 2.3$ in year 2000 to $M_c \approx 1.9$ in the year 2006 [*Amato and Mele*, in print]. The number and quality of installed stations increased from about 100 short-period vertical instruments at the end of the 1990s to more than 250, mostly three-component seismometers at the end of 2007. At this time, the RSN was connected to more than 150 broad-band and very-broad-band instruments (Streckeisen STS-1 and STS-2, Güralp CMG 40 and 360, Trillium 40 and 120), and about 100 short period instruments (Teledyne GeoTech S13, Kinemetrics SS1-Ranger, Mark L-4C, and Lennartz LE3D 1/5/20 S).

Today, the RSN receives signals from more than 270 stations belonging to the Italian National Seismic Network [*Amato et al.*, 2006], the MedNet Seismic Network [*Mazza et al.*, 2008], the Swiss Digital Seismic Network [*Baer et al.*, 2000], the French Broad-band Seismological Network [*Granet*, 2001], the Austrian Seismic Network [*Lenhardt and Melichar*, 2000], the Hellenic Broadband Seismological Network [*Melis and Konstantinou*, 2006], the Slovenian National Seismic Network [*Kobal et al.*, 2007], and from five regional Italian networks. The rapid development of the RSN started in 2001 with the first triennial agreement between the INGV and the Dipartimento della Protezione Civile (Italian Civil Protection Department, DPC), recently renewed until 2010, and was also partly supported in southern Italy by the PROSIS project funded by the Italian Ministry of Research.

The RSN was centralized in the early 1980s, soon after the destructive 1980 Irpinia earthquake. An automatic acquisition system [*Taccetti et al.*, 1989], connected with analog telephone lines, was able to locate earthquakes in Italy since 1984, exploiting the signals of, at its maximum extent, 100 short-period stations. A new acquisition system, fully operational since 2004, connected with digital terrestrial and satellite lines, provides first rapid locations within 20–30 seconds from the origin time, first evaluation of M_L magnitudes within 40 seconds, and final locations and magnitudes with a delay ranging from three to five minutes after the origin time. More than 75% of the earthquakes are automatically located in real-time within 10 km from the revised locations in the bulletin, whereas the real-time magnitudes M_L are within ± 0.4 magnitude units from the revised values in 90% of the cases [*Amato and Mele*, in print].

The current agreement between INGV and the Civil Protection Department contemplates three different levels of communications: the personnel in charge for seismic surveillance reports an estimate of the area struck by any earthquake in Italy within two minutes after the origin time; the first evaluations of the location and magnitude are communicated within five minutes, while the definitive revised hypocentral parameters are computed and communicated with a maximum delay of 30 minutes.

The sparse short period network, whose installation started in the early 1980s, was the main source of information for the Bollettino Sismico Italiano (Italian Seismic Bulletin, BSI) until April 2005. The data collected in the old BSI were integrated with parametric data produced by other local Italian seismic networks and published as the Catalogo Strumentale dei Terremoti Italiani dal 1981 al 1996 (Instrumental Catalog of Italian Earthquakes from 1981 to 1996, CSTI) [*Augliera et al.*, 2001], and successive revisions [*CSTI Working Group*, 2004]. A later integration of the BSI with data from other networks was published in the Catalogo della Sismicità Italiana 1981–2002 (Catalog of Italian Seismicity 1981–2002, CSI 1.1) [*Castello et al.*, 2006; *Chiarabba et al.*, 2005].

Since 16 April 2005, new tools for interactive analysis of seismic data became fully operational [*Bono and Badiali*, 2005]. After then, the BSI includes data from the whole RSN [*Mele et al.*, 2007]. The renewed BSI located 6058 earthquakes during 2006 (in the area 36°N–48°N, 6°E–19°E) and 5954 earthquakes in 2007, while the old BSI counted only 1885 earthquakes in the same area in 2004.

Before 16 April 2005, the BSI included low local magnitude values ($M_{\mathrm{L}} < 3$) computed approximating the Wood-Anderson pick-to-pick maximum elongation with the maximum elongation registered on short period (one second) vertical signals. For earthquakes with $M_{\mathrm{L}} \geq 3$, the magnitude was computed by the MedNet broad-band network [*Mazza*, 1996; *Mazza et al.*, 1998]. In the old BSI, only 70% of the earthquakes had an M_{L} value assigned, the reminder being classified with duration magnitudes only. *Gasperini* [2002] drew a detailed picture of the history of magnitude computation at INGV in the period 1981–1996. He also made a strong effort in trying to homogenize the magnitude values included in the CSTI using data from very different sources (short-period vertical amplitudes, short-period duration magnitudes, synthetic Wood-Anderson seismograms from broad-band records and some true Wood-Anderson amplitudes), and computed a new analytical attenuation law and station magnitude residuals, as proposed by *Hutton and Boore* [1987]. *Castello et al.* [2007] derived duration magnitude and station correction estimates for the entire CSI catalog through a linear regression between local magnitudes calculated from synthetic Wood-Anderson (with the MedNet broad-band seismometers) and the corresponding short-period seismic-signal durations at the RSN.

Method

We apply the method for probabilistic estimates of recording completeness developed by *Schorlemmer and Woessner* [2008]. A detailed description of this method can be found in their publication. As described in the Introduction, this method avoids most of the assumptions that traditional completeness-estimation methods make. It uses empirical data only: (1) the earthquake catalog with phase-pick information, (2) the station list and information about on- and off-times of stations, and (3) the attenuation relation used for computing magnitudes. Here, we give only a brief description of this method:

In a first step, we derive per station a distribution over magnitude and distance of probabilities of detecting earthquakes. For calculating a detection probability for a particular magnitude and distance to the station, we select all events of the respective magnitude and distance to the station. We only select events that occurred during periods in which the station was operating. Furthermore, we have to add a range to the magnitude and distance values for sampling. This range is determined by the attenuation relation, see [*Schorlemmer and Woessner*, 2008]. From such a set of earthquakes, we calculate the detection probability as the ratio of the number of detected events over the total number of events. Repeating this procedure for the full range of magnitudes and distances leads to a full probability distribution for a station. This distribution is smoothed by applying two simple physical constraints, detection probabilities cannot become lower for smaller distances at the same magnitude and for larger magnitudes at the same distance, respectively. This algorithm removes artifacts that stem from sparse data. The computation of detection probabilities is not truly mimicing the network operation as we use $P_{\mathrm{D}}(\mathrm{A}|\mathrm{B})$ instead of $P_{\mathrm{D}}(\mathrm{A})$, where P_{D} is the probability that an event with magnitude M at a distance L is detected at a particular station. Here A means that the earthquake triggered the station and B that the earthquake triggered a sufficient number of stations to be localized. This could potentially cause overestimated detection probabilities for small magnitude earthquakes close to the station. Such an event would only be detected by the neareast stations and in case of one station missing it, it would not appear in the catalog, thus not contributing to the computations of detection probabilities. Therefore, $P_{\mathrm{D}}(\mathrm{A})$ is not a directly accessible quantity; however, we show below that it can be approximated by $P_{\mathrm{D}}(\mathrm{A}|\mathrm{B})$ without introducing a significant bias.

The detection-probability distributions describe the detection characteristic of each station in the network, and because they are derived from a catalog spanning a multi-year period, no significant changes in recording should occur during this period. Possible changes include changes of the magnitude definition, the triggering algorithm, or the occurrence of large aftershock sequences during which completeness may vary [*Helmstetter et al.*, 2006; *Enescu et al.*, 2007]. All recording-completeness estimates are further derived from these probability distributions.

In a second step, we compute the probabilities of recording of an event with a particular magnitude for a set of points in space for a given time, e. g., a grid on a map or a cross-section. For that purpose, we identify all stations that were in operation at this particular time. For each of the stations, we compute the distance to the point in space and estimate the detection probability from the probability distributions. The probability of the network to detect an event of the given magnitude at this point in space is the combined probability that four or more stations have detected it. This number reflects the condition of the INGV system to notify the operators of a potential earthquake signal (triggering).

Repeating this computation for the full range of magnitudes provides a description of detection probabilities for each point in space and magnitude. From this description, we derive completeness values for each point in space by searching the smallest magnitude that exhibits the desired detection probability, $P_{\mathrm{E}} = 0.999$, that we consider representing completeness. This corresponds to a miss rate of one in thousand events.

To investigate network failure scenarios, we compute completeness maps based on a limited set of stations; we remove either stations that are connected through a specific link (Internet, VPN, or satellite) or use only stations that are linked by satellite to the center. The first scenario accounts for failures of systems linking stations to the operational center, the second simulates operation in a second available center that receives data only through the satellite link.

To address the aforementioned bias, we have to show that $P_{\mathrm{D}}(\mathrm{A}|\mathrm{B}) = P_{\mathrm{D}}(\mathrm{A})$, or at least very similar such that the difference is not significantly affecting subsequent results, for events with magnitudes equal to or larger than the completeness magnitude. Let us define $P_i(\mathrm{A}|L, M)$ as the probability that an event of magnitude M at a distance L triggers the ith station, $P_i(\mathrm{A}|L, M, \mathrm{B})$ is the same probability conditioned by the fact that the event is localized, and $P_i(\mathrm{A}|L, M, \underline{\mathrm{B}})$ is the same probability conditioned by the fact that the event is not localized. Basically, we want to prove the hypothesis $\mathcal{H}$, i.e., $P_i(\mathrm{A}|L, M) = P_i(\mathrm{A}|L, M, \mathrm{B})$.

The difference between localized and non-localized events simply relies on the number of stations that detect the event. In other words, a localized earthquake is detected by at least $N_{\rm loc}$ stations, while a non-localized event is detected by less than N_{loc} stations or even none. In order to verify our hypothesis $\mathcal{H}$, we assume that the 'localized' (B) events are the ones recorded at $N_{\rm loc}$ or more stations and that the events localized by only $N_{\rm loc} - 1$ or less stations are 'non-localized' events ($\underline{\rm B}$). We necessarily neglect all events not recorded by any stations because they are uncountable by definition. For large magnitude events, the number of undetected events will be obviously negligible, but it may become important for small magnitude earthquakes. Here, we assume that this number is negligible for the magnitude range considered in this paper. In other words, we assume that the no events above the final completeness magnitude can be completely undetected. Note that the this assumption is implicitly verified if the hypothesis $\mathcal{H}$ turns out to be realistic. In fact, if $\mathcal{H}$ holds, this implies also that the number of undetected event is negligible for the magnitudes of interest.

We verify the reliability of $\mathcal{H}$ in two different ways. At first, if our hypothesis $\mathcal{H}$ is true, we expect that the detection capability of a station does not change significantly if we consider events detected by a different number of stations. In Figure @@ we report the standardized differences between the detection probability for $N_{\rm loc}$=4-5, 4-6, and 4-7, for two selected stations. Estimates and uncertainties are calculated assuming a binomial distribution in each $L - M$ bin. The figure shows that the detection probability of each station does not vary significantly with $N_{\rm loc}$ for magnitudes larger than the completeness magnitude (vertical dotted line) as expected if our hypothesis $\mathcal{H}$ is true. Note that we use low $N_{\rm loc}$ because high values of $N_{\rm loc}$ would involve only large magnitude events.

The second check consists of looking at the detection capability for all stations simultaneously. The probabilities of interest for the whole range of L and M ($\sum_{L,M} P_i({\rm A}|L, M)$

and $\sum_{L,M} P_i(\mathrm{A}|L,M,\mathrm{B}))$ can be approximated by

$$\sum_{L,M} P_i(\mathrm{A}|L,M,\mathrm{B}) \equiv P_i(\mathrm{A}|\mathrm{B}) = N_+/N_{\mathrm{tot}} \tag{1}$$

$$\sum_{L,M} P_i(\mathrm{A}|L,M) \equiv P_i(\mathrm{A}) = N_+^*/N_{\mathrm{tot}}^* \tag{2}$$

where N_+ is the number of localized events recorded at the ith station station, while N_+^* is the number of events recorded at that station. Similarly, N_{tot} is the number of localized events and N_{tot}^* the number of recorded events (localized or not). As before, N_{tot}^* should contain also the non detected earthquakes that are impossible to count, but we assume that the number of such events is negligible for the magnitude range of interest (see above).

Let us define the number of non-localized events recorded at the station as $\Delta N_+ \equiv N_+^* - N_+$, and the number of non-localized events as $\Delta N_{\mathrm{tot}} \equiv N_{\mathrm{tot}}^* - N_{\mathrm{tot}}$. Using equations 1 and 2, $P_i(\mathrm{A})$ can be reformulated as

$$P_i(\mathrm{A}) = P_i(\mathrm{A}|\mathrm{B})[(1 + \Delta N_+/N_+)/(1 + \Delta N_{\mathrm{tot}}/N_{\mathrm{tot}})] \tag{3}$$

Therefore, the condition that $P_i(\mathrm{A}|\mathrm{B}) = P_i(\mathrm{A})$ is met if

1. $\Delta N_+ = 0$ and $\Delta N_{\mathrm{tot}} = 0$ or if
2. $N_+/N_{\mathrm{tot}} = \Delta N_+/\Delta N_{\mathrm{tot}}$, i. e., when $P_i(\mathrm{A}|\mathrm{B}) = \Delta N_+/\Delta N_{\mathrm{tot}}$.

The first case can be considered the trivial case and should only apply to larger magnitudes for which the catalog is complete. The second case implies that the percentage of non-localized events recorded at a station is similar (equal to) the percentage of localized events recorded at that station. In other words, the localized events can be seen as a random sample of the entire distribution.

To verify this claim, we compare the detection probability for localized and non-localized events per all stations using events with magnitude 2.5 or larger that is a reasonable completeness value for most of the italian territory (see below). For each station in the network, we compute the frequency of events detected by $N_{\mathrm{loc}} - 1$ stations or less, and N_{loc} or more stations. In particular, for each station we estimate 1) the percentage of earthquakes detected by N_{loc} or more stations that are also detected by the station under consideration; 2) the percentage of earthquakes detected by $N_{\mathrm{loc}} - 1$ or less stations that are also detected by the station under consideration. These frequencies can also be interpreted as probabilities that an event which is recorded by $N_{\mathrm{loc}} - 1$ or less, or N_{loc} or more stations is detected at the particular station. Because events are recorded at multiple stations, the sum over all probabilities at all stations for one event is more than 1, since it represents the average number of stations recording a nonlocalized (the average number of stations is M_1) and localized (the average number of stations is M_2) event in the INGV network. These probabilities are not comparable as they are, but they have to be multiplied by the probability that the ith station is one of the triggered station, i.e., $1/M_1$ for nonlocalized events, and $1/M_2$ for localized events.

If the hypothesis $\mathcal{H}$ ($P_i(\mathrm{A}|\mathrm{B}) = P_i(\mathrm{A})$) holds, the latter probabilities should be the same for the case that events were detected at $N_{\mathrm{loc}} - 1$ or less stations and the case that events were detected at N_{loc} or more stations. For each station, we calculate a z-value, subtracting these probabilities and normalizing them with the square root of the sum of the two variances for the cases $N_{\mathrm{loc}} = 10, 13, 15$. We choose these values because the average number of stations recording a M 2.5 event is about 14. If the differences between the percentages are not statistically significant, we would expect to see less than

1% of these values above $z = 2.5$ or below $z = -2.5$ that represents the 99% confidence interval. For all N_{loc} considered we never have more than 1% of the differences outside this interval. This confirms that difference in the percentages is not statistically significant for earthquakes above the completeness magnitude, and consequently it confirms the reliability of our hypothesis $\mathcal{H}$. In practice, using $P_i(\mathrm{A}|\mathrm{B})$ instead of $P_i(\mathrm{A})$ does not introduce any significant bias into the completeness analysis.

Data

As described previously, 16 April 2005 marks the starting date of the new generation of the Italian network. We use the earthquake catalog from 16 April 2005 to 1 January 2008. During this period, 14722 events were located. The complete data set has been used in this analysis. Figure 1 shows the distribution of earthquake activity in Italy during this period. 95% of the events have depths of less than or equal 30 km. Only in the Tyrrhenian Sea a significant number of events has larger depths of up to 500 km. The catalog contains no significant aftershock sequences as only two events have magnitudes larger than 5 ($M = 5.4$ and $M = 5.7$). Most of the seismicity is distributed along the Apennines mountain chain, around the Strait of Messina, and in the Tyrrhenian Sea.

For correct characterizations of stations, the knowledge of station off-times is crucial; If not taken into account, the performance of a station will be affected by missed events which occurred during off-times but may have been recorded if the station had been in operation. Although the INGV database provides off-time entries, mostly due to maintenance or serious failures, the average short-time failures are not included and not updated by the operators. We derive approximate off-times by waveform-file lists. The INGV stores a waveform file for each hour-block and each station channel. If such a file is missing for a given one-hour period, we consider this period as off-time of the channel. Although scanning through the waveform-files for identifying periods of missing signals is certainly superior, we, for computational reasons, defined the off-times by missing of the according waveform-files.

Both, CSTI and CSI catalogs, include heterogeneous magnitude values. The new BSI (since 16 April 2005) covers only three years of data but is a seismic catalog unprecedented in Italy for completeness and homogeneity in the computation of local magnitudes. The M_{L} magnitude evaluation follows a standard procedure: M_{L} have been routinely computed using a full Wood-Anderson signal reconstruction from broad-band horizontal records [*Kanamori and Jennings*, 1978], with the exception of a few small earthquakes, 3% of the total, classified with M_{d} only, recorded by short period vertical instruments or with broad-band records affected by gaps. Two attenuation laws were computed for northwestern Italy [*Bindi et al.*, 2005] and for northeastern Italy [*Bragato and Tento*, 2005]. The only (M_{L}) attenuation law available for entire Italy relies on a very limited set of data [*Gasperini*, 2002]. Therefore, the network maintainers chose to use the attenuation law proposed by *Hutton and Boore* [1987] for California:

$$-\log A_0 = 1.110\log(r/100) + 0.00189(r-100) + 3.0 \tag{4}$$

where $-\log A_0$ is the distance correction used in the original definition by *Richter* [1958] and r is the hypocentral distance in kilometers. Therefore, the event magnitude, M_{L}, is defined as

$$M_{\mathrm{L}} = \log A + 1.110\log(r) + 0.00189r + 3.591 \tag{5}$$

where A is the Wood-Anderson amplitude in meters. The magnitude is computed as trimmed mean of the available station magnitudes, following the algorithm of *Huber* [1981] to eliminate the outliers.

All stations are connected to the Centro Nazionale Terremoti (National Earthquake Center, INGV-CNT) in Rome with four main links: 1) a satellite link by means of two main providers, INTELSAT and HELLASAT (98 stations, 288 channels); 2) a shared public internet connection (37 stations, 99 channels); 3) a Virtual Private Network (VPN) 'point to point' link (60 stations, 180 channels); 4) other, mostly analog links through telephone leased lines (60 stations, 76 channels). In the near future, INGV is planning to create a mirror of the seismic data collected through the satellite link in another INGV department to be able to continue earthquake recordings in case of a complete failure of the main INGV-CNT in Rome.

Results

We computed maps of detection probability, P_{E}, for magnitudes 0–4 in 0.1 magnitude unit steps for 1 January 2008 and a depth layer of 30 km (see a selection of maps in Figure 2). We have chosen 30 km as our target depth layer because 95% of all earthquakes in the catalog are located with depths between 0 and 30 km. At 1 January 2008, the network was able to record $M = 1$ events with a probability of $P_1 \approx 0.7$ ($P_1 \equiv P_{\mathrm{E}}(M, \mathbf{x})|_{M_{\mathrm{L}}=1}$, same for other magnitudes) in the central Apennines, at locations in the southern Apennines, and with slightly reduced probability in Switzerland's south-eastern canton Graubünden due to reporting stations there. In all other parts of Italy, the network is not able to record events of such small magnitude as the station density is lower than in the aforementioned three regions (Figure 2A). With increasing magnitude, the detection probabilities increase mostly along the central and southern Apennines but also in the northern and western parts of the Italian Alps. In the Basilicata and Campania regions P_{E} reaches the 0.999 level for $M = 1.5$, rendering this area the one with lowest completeness magnitude in Italy (Figure 2B). Further increasing the magnitude is increasing the detection probabilities along the Apennines chain and the Italian Alps. For magnitude $M = 2$ these areas are mostly complete at the $P_{\mathrm{E}} = 0.999$ level. In the coastal areas of Liguria, Tuscany, and Lazio on the west coast and of Veneto and Emilia-Romagna on the east coast, detection probabilities are below the completeness level. Further areas of lower detection probabilities are Apulia and Sicily which partly do not show any coverage of $M = 2$ events. The islands of Sardinia, Pantelleria, and Lampedusa do not exhibit any noticeable detection probability at the $M = 2$ level (Figure 2C).

Completeness at the $P_{\mathrm{E}} = 0.999$ level is reached for most of Italy at magnitude $M = 2.5$ (Figure 2D). The southern parts of Apulia and the western part of Sicily have detection probabilities at the $P_{\mathrm{E}} \approx 0.8$ level. Again, the islands of Sardinia, Pantelleria, and Lampedusa are not covered at any noticeable probability level. Magnitude $M = 2.5$ is the reporting threshold level of the Italian Civil Protection because it represents the minimum magnitude that can be clearly detected by the population, and that may raise some concerns from inhabitants and/or local authorities. Completeness at the $P_{\mathrm{E}} = 0.999$ level for the entire mainland of Italy including Sicily is reached at $M = 2.9$ (Figures 2E and 2F).

We also computed completeness maps for different probability levels and different depth layers (Figure 3). We have chosen probability levels of $P_{\mathrm{E}} = 0.99$ and $P_{\mathrm{E}} = 0.99999$ and depth levels of 0 km, 15 km, and 60 km. The additional probability levels correspond to a 1% and 0.001% chance of missing an event. As expected, completeness magnitudes are lower for the lower probability level $P_{\mathrm{E}} = 0.99$. Simultaneously, they are higher for $P_{\mathrm{E}} = 0.99999$. We have chosen to display completeness magnitudes with a rather coarse and discrete colormap to better visualize the changes in completeness with changing parameters.

A similar trend can be seen for varying depth layers. We additionally computed completeness magnitudes M_{P} for depth layers of 0 km, 15 km, and 60 km. Because the completeness depends directly on the distance of the hypocenter to the station, completeness magnitudes are increasing with increasing depth.

This trend can also be seen in the detection-probability cross-sections in Figure 4. Detection probabilities are increasing with increasing magnitudes first below the mainland of Italy (the Apennines). For magnitude 1.5, shallow earthquakes can also be detected below Sicily. The network is very reliably detecting magnitude $M = 2$ earthquakes below the landmass down to a depth of 50 km, and down to 100 km for magnitude $M = 2.5$. For magnitude $M = 2.9$, reliable detection can also be seen at about latitude 46°N, which corresponds to the Friuli region. Compiling these results into a completeness cross-section shows the gradual decrease in completeness (increasing magnitude values) with depths and the two most complete area below the mainland of Italy and below Sicily.

We investigated the effect of major system failures to the detection capability of the network. The most likely failure scenario is a malfunction of a telemetry link between stations and the operating center. We computed four possible scenarios: Outage of the Internet link, outage of the VPN connection, outage of the satellite link, and a scenario in which only the satellite link is available. Although the INGV-CNT is connected to two satellites, an outage of both satellite connections is the more likely scenario. Heavy rain in Rome can prevent reception of useful data from the satellite. It can cause a rapid growth of packet retransmission requests to stations which leads to a saturation of the bandwidth dedicated to each station. This results in signals with unrecoverable gaps or larger delays that might prevent the signals to be useful for magnitude computations or even locations. Another reason for this scenario is the possible failure of the computer managing both satellite connections. The last scenario corresponds to a complete failure of the operating center in Rome. We computed this scenario as a simulation for a future datacenter mirroring the INGV-CNT but having only access to station data connected via satellite. Figure 5 summarizes the changes in detection probabilities and completeness magnitudes.

All three scenarios that correspond to a failure of one telemetry link show only a slight loss in completeness. In case the Internet connection is lost, the main loss occurs on the northern edge of the network coverage, especially in Switzerland. All stations in Switzerland are connected through the Internet to the operating center in Rome and, thus, a failure would most strongly affect this region. Missing station data of stations in center regions of the network has not a similarly strong effect as they can more easily be compensated by other stations. If the stations are on the edge of the network, the detection probability drops significantly. Failure of the VPN connection also shows a drop in the northern part of the network, although a smaller one. The detection probabilities in southern Italy are not affected significantly. In contrary, if the satellite link fails, detection probabilities are strongly affected in southern Italy, especially in Apulia and Sicily. The strong dependence on the satellite link for earthquake detection in southern Italy can also be seen in the last scenario, in which only the satellite link is functioning. While southern Italy still exhibits detection probabilities comparable to the undisturbed case, the network is strongly losing its detection capability in northern Italy.

Discussion and Conclusion

Completeness studies of seismic catalogs represent the cornerstone of any reliable statistical analysis of earthquake catalog data. Not only direct measures of catalog properties, like seismic rate changes or earthquake-size distributions, depend strongly on complete datasets, but also evaluations of earthquake forecasting models and the models themselves. For example, the use of incomplete catalogs can easily lead to overestimate the forecasting capability of any model [*Marzocchi et al.*, 2003].

Here, we present a detailed study of the completeness of the INGV bulletin since April 2005. The basic prerogative of the method is that it relaxes most of the assumptions that stand behind previous techniques [*Schorlemmer and Woessner*, 2008], and it relies on the detection capability of each station of the seismic network. The results reported here have many potential applications. Three of them are particularly relevant:

– It provides the threshold magnitude over space and time, and therefore a complete seismic catalog that can be used for different purposes.

– It gives a real-time picture of the INGV seismic network detectability. This is of paramount importance for selecting areas where the network should be improved, and to have a realistic view of the network detectability during a major failure of one or more connections to the stations. The results reported here, for instance, emphasize the importance to improve the satellite link coverage, overall in northern Italy.

– It provides a framework to establish a rigorous quantitative evaluation of forecasting models applied in a forward perspective.

The results reported here show a substantial improvement of the recent seismic network capability compared to the past. Besides providing earthquake information in almost real-time, it gives also sufficient information to explore the space-time variation of the network detectability. This cannot be done using past catalogs and bulletins. In particular, we show that a magnitude of 2.5 can be used as a reasonable threshold for most of the territory, and in some regions, this threshold reaches a value close to 1.0.

The failure scenario computations highlight the stability of the network. None of the single link failures does affect the detection probability of the network so strongly that a significant completeness drop would occur. Only along the edges of the network coverage, drops in completeness are reducing the extent of the coverage.

In the near future, INGV is planning to create a mirror for data collected through the satellite link. Further plans are to improve the data exchange with neighboring countries, e. g., with France and Greece. As a result of this study, INGV is further planning to improve the network coverage in the regions where the earthquake detectability is lower (e. g., western Sicily). INGV will install the programs used to perform this study at the INGV-CNT data center, for monitoring the earthquake detectability of the network as a function of the daily status of the stations and connections.

As a final remark, we note that the method used here has two paramount prerogatives compared to techniques usually applied for Italian territory. First, it allows to drop the assumption of stationarity in seismicity that stands behind some models frequently used in Italy [*Tinti and Mulargia*, 1985]. As a matter of fact, recent studies show that long-term modulation of seismicity may be ubiquitous and not due to under-reporting of seismic catalogs [*Selva and Marzocchi*, 2005; *Lombardi and Marzocchi*, 2007]. Second, even assuming that a Gutenberg-Richter law holds for Italian seismicity, the results reported here show significant spatial heterogeneity of the seismic completeness that could lead to some biases on estimating completeness threshold magnitudes through the use of the Gutenberg-Richter law on the whole catalog.

Acknowledgments. We thank Raffaele di Stefano for waveform-file listings for obtaining station off-times of the INGV network. In particular, we want to thank the open-source community for the Linux operating system and the many programs used in this study. Maps were created using GMT [*Wessel and Smith*, 1991]. All input data and all codes needed to reproduce the results of this study are available on the website `www.completenessweb.org`. All completeness data can be downloaded there. The RSN has been partly developed with the financial support of the Italian *Dipartimento della Protezione Civile* (Department of Civil Protection of the National Ministry Council). This research was supported by the NSF-EAR-0738785 grant and the Southern California Earthquake Center (SCEC). SCEC is funded by NSF Cooperative Agreement EAR-0106924 and USGS Cooperative Agreement 02HQAG0008. The SCEC contribution number for this paper is 1219. This project was in parts supported by the European Union project NERIES (contract number 026130).

References

Amato, A., and F. M. Mele (in print), Performance of the INGV National Seismic Network from 1997 to 2007, *Annals of Geophysics*.

Amato, A., L. Badiali, M. Cattaneo, A. Delladio, F. Doumaz, and F. M. Mele (2006), The real-time earthquake monitoring system in Italy, *Géosciences (BRGM)*, *4*, 70–75.

Amorèse, D. (2007), Applying a change-point detection method on frequency-magnitude distributions, *Bull. Seismol. Soc. Am.*, *97*, 1742–1749, doi:10.1785/0120060181.

Augliera, P., et al. (2001), Catalogo Strumentale dei Terremoti Italiani dal 1981 al 1996 (CSTI), Versione 1.0, CD-ROM.

Baer, M., P. Zweifel, and D. Giardini (2000), The Swiss Digital Seismic Network (SDSNet), *ORFEUS Newsletter*, *2*(2), 10.

Bindi, D., D. Spallarossa, C. Eva, and M. Cattaneo (2005), Local and duration magnitudes in northwestern Italy, and seismic moment versus magnitude relationships, *Bull. Seismol. Soc. Am.*, *95*(2), 592–604.

Bono, A., and L. Badiali (2005), PWL Personal Wavelab 1.0, an object-oriented workbench for seismogram analysis on Windows systems, *Computers & Geosciences*, *31*(1), 55–64.

Bragato, P. L., and A. Tento (2005), Local magnitude in northeastern Italy, *Bull. Seismol. Soc. Am.*, *95*(2), 579–591.

Cao, A., and S. S. Gao (2002), Temporal variation of seismic *b*-values beneath northeastern Japan island arc, *Geophys. Res. Letts.*, *29*(9), 1334, doi:10.1029/2001GL013775.

Castello, B., G. Selvaggi, C. Chiarabba, and A. Amato (2006), CSI Catalogo della Sismicità Italiana 1981–2002, Versione 1.1, http://legacy.ingv.it/CSI/, istituto Nazionale di Geofisica e Vulcanologia, Roma.

Castello, B., M. Olivieri, and G. Selvaggi (2007), Local and duration magnitude determination for the Italian earthquake catalog, 1981–2002, *Bull. Seismol. Soc. Am.*, *97*, 128–139.

Chiarabba, C., L. Jovane, and R. D. Stefano (2005), A new view of Italian seismicity using 20 years of instrumental recordings, *Tectonophysics*, *395*, 251–268.

CSTI Working Group (2004), Catalogo Strumentale dei Terremoti Italiani dal 1981 al 1996, Versione 1.1, `http://ibogfs.df.unibo.it/user2/paolo/www/gndt/Versione1_1/Leggimi.htm`.

Enescu, B., J. Mori, and M. Miyazawa (2007), Quantifying early aftershock activity of the 2004 mid-niigata prefecture earthquake (*mw* 6.6), *J. Geophys. Res.*, *112*, B04310, doi:10.1029/2006JB004629.

Enescu, B., J. Mori, M. Miyazawa, and Y. Kano (in print), Omori-utsu law *c*-values associated with recent moderate earthquakes in japan, *Bull. Seismol. Soc. Am.*

Gasperini, P. (2002), Local magnitude revaluation for recent Italian earthquakes (1981–1996), *J. Seism.*, *6*(4), 503–524.

Gomberg, J. (1991), Seismicity and detection/location threshold in the southern Great Basin seismic network, *J. Geophys. Res.*, *96*(16), 16,401–16,414.

Granet, M. (2001), The French National Network of Seismic Survey (RéNaSS), *ORFEUS Newsletter*, *3*(1), 2.

Gutenberg, B., and C. F. Richter (1944), Frequency of earthquakes in California, *Bull. Seismol. Soc. Am.*, *34*, 185–188.

Helmstetter, A., Y. Y. Kagan, and D. D. Jackson (2006), Comparison of short-term and long-term earthquake forecast models for southern california, *Bull. Seismol. Soc. Am.*, *96*, 90–106.

Huber, P. J. (1981), *Robust statistics*, Wiley, New York.

Hutton, L. K., and D. M. Boore (1987), The M_{L} scale in southern California, *Bull. Seismol. Soc. Am.*, *77*(6), 2074–2094.

Ishimoto, M., and K. Iida (1939), Observations of earthquakes registered with the microseismograph constructed recently, *Bull. Earthquake Res. Inst. Tokyo Univ.*, *17*, 443–478.

Kanamori, H., and P. C. Jennings (1978), Determination of local magnitude, m_l, from strong-motion accelerograms, *Bull. Seismol. Soc. Am.*, *68*, 471–486.

Kobal, M., J. Kolar, J. Pahor, and M. Živčić (2007), Performance of the seismic network of the Republic of Slovenia, first results, *ORFEUS Newsletter*, *7*(2).

Kvaerna, T., F. Ringdal, J. Schweitzer, and L. Taylor (2002a), Optimized seismic threshold monitoring – Part 1: Regional processing, *Pure Appl. Geophys.*, *159*(5), 969–987.

Kvaerna, T., F. Ringdal, J. Schweitzer, and L. Taylor (2002b), Optimized seismic threshold monitoring – Part 2: Teleseismic processing, *Pure Appl. Geophys.*, *159*(5), 989–1004.

Lenhardt, W., and P. Melichar (2000), The Austrian Seismic Network, *ORFEUS Newsletter*, *2*(3), 20.

Lombardi, A. M., and W. Marzocchi (2007), Evidence of clustering and nonstationarity in the time distribution of large worldwide earthquakes, *J. Geophys. Res.*, *112*, B02303, doi:10.1029/2006JB004568.

Marsan, D. (2003), Triggering of seismicity at short timescales following Californian earthquakes, *J. Geophys. Res.*, *108*(B5), 2266, doi:10.1029/2002JB001946.

Marzocchi, W., L. Sandri, and E. Boschi (2003), On the validation of earthquake-forecasting models: The case of pattern recognition algorithms, *Bull. Seismol. Soc. Am.*, *93*(5), 1994–2004.

Mazza, S. (1996), Magml, Programma per il Calcolo della Magnitudo M_{L} da dati broad-band, *Open File, Istituto Nazionale di Geofisica, Roma.*

Mazza, S., A. Morelli, and E. Boschi (1998), Near real-time data collection and processing at MEDNET, *Eos Trans. AGU*, *79*, 569.

Mazza, S., M. Olivieri, A. Mandiello, and P. Casale (2008), The Mediterranean Broad Band Seismographic Network Anno 2005/06, in *Earthquake Monitoring and Seismic Hazard Mitigation in Balkan Countries*, *NATO Science Series*, vol. 81, edited by E. S. Husebye, pp. 133–149, Springer Netherlands, doi:10.1007/978-1-4020-6815-7.

Mele, F. M., C. Marcocci, R. Moro, D. Riposati, and B. Castello (2007), ISIDe, the Italian Seismic Instrumental and Parametric Data Base (Bollettino Sismico Italiano), `http://iside.rm.ingv.it/`, istituto Nazionale di Geofisica e Vulcanologia, Roma.

Melis, N. S., and K. I. Konstantinou (2006), Real-time seismic monitoring in the Greek region: An example from the 17 october 2005 east Aegean Sea earthquake sequence, *Seismol. Res. Letts.*, *77*(3), 364–370.

Richter, C. F. (1958), *Elementary Seismology*, W. H. Freeman and Company.

Rydelek, P. A., and I. S. Sacks (1989), Testing the completeness of earthquake catalogues and the hypothesis of self-similarity, *Nature*, *337*, 251–253.

Schorlemmer, D., and J. Woessner (2008), Probability of detecting an earthquake, *Bull. Seismol. Soc. Am.*, *98*(5), 2103–2117, doi:10.1785/0120070105.

Selva, J., and W. Marzocchi (2005), Variations of Southern California seismicity: empirical evidence and possible physical causes, *J. Geophys. Res.*, *110*, B11306, doi:10.1029/2004JB003494.

Taccetti, Q., F. M. Mele, and R. Buland (1989), Il sistema automatico per la rilevazione, il processamento e l'archiviazione dei dati della rete sismica nazionale italiana I. N. G., in *Aree sismogenetiche e rischio sismico in Italia - II*, edited by E. Boschi and M. Dragoni, pp. 1–7, Il Cigno Galileo Galilei, Lausanne, in Italian.

Tinti, S., and F. Mulargia (1985), Completeness analysis of a seismic catalog, *Annales Geophysicae*, *3*(3), 407–414.

Wessel, P., and W. H. F. Smith (1991), Free software helps map and display data, *Eos Trans. AGU*, *72*(441), 445–446.

Wiemer, S., and M. Wyss (2000), Minimum magnitude of completeness in earthquake catalogs: Examples from Alaska, the western United States and Japan, *Bull. Seismol. Soc. Am.*, *90*(4), 859–869.

Woessner, J., and S. Wiemer (2005), Assessing the quality of earthquake catalogues: Estimating the magnitude of completeness and its uncertainty, *Bull. Seismol. Soc. Am.*, *95*(2), 684–698, doi:10.1785/0120040007.

Figure 1. Seismicity map of Italy. Squares indicate earthquakes of the catalog from the period 16 April 2005 to 1 July 2008. The size and color of the squares indicate the magnitude and hypocentral depth of the events, respectively. Most of the recorded events are located along the Apennines, the Tyrrhenian Sea, and the Strait of Messina. The deep events are located along the subduction slab in the Tyrrhenian arc. The vertical bars indicate the extension of the cross-section shown in Figure 4.

Figure 2. Map of detection probabilities, P_{E}, for different magnitudes on 1 January 2008 at a depth of 30 km. (top left) Map of P_1. (top center) Map of $P_{1.5}$. Gray triangles mark all stations that were in operation on 1 January 2008. (top right) Map of P_2. Gray boxes mark all earthquakes of magnitude $M = 2$ that ocurred during the period 16 April 2005–1 January 2008. (bottom left) Map of $P_{2.5}$. Magnitude $M_{\mathrm{L}} = 2.5$ represents the reporting threshold level of the Italian Civil Protection. The black contour lines indicate the $P_{2.5} = 0.99$ and $P_{2.5} = 0.999$ level. (bottom center) Map of $P_{2.9}$. The catalog can be considered complete at the $M_{\mathrm{P}} = 2.9$ level for the entire territory of Italy except for the islands of Sardinia, Pantelleria, and Lampedusa. Contour lines as in frame D. (bottom right) Map of M_{P} at the $P = 0.999$ level. The white contour lines show the $M_{\mathrm{P}} = 2.5$ contour (inner line) and $M_{\mathrm{P}} = 2.9$ contour (outer line).

Figure 3. Maps of completeness magnitude, M_{P}, for different probability levels and different depth layers. The M_{P}-values are plotted in 0.5 magnitude contour levels to highlight the changes with changing parameter. Top row shows how the M_{P}-values are rising with higher probability levels at the depth layer of 30 km. (top left) M_{P} at the $P = 0.99$ level. (top center) M_{P} at the $P = 0.999$ level. (top right) M_{P} at the $P = 0.99999$ level. Bottom row shows how M_{P}-values are rising with higher depth at the probability level of $P = 0.999$. (bottom left) M_{P} at 0 km depth. (bottom center) M_{P} at 15 km depth. (bottom right) M_{P} at 60 km depth.

Figure 4. Cross-section of detection probabilities, P_{E}, for different magnitudes on 1 January 2008 along 15°E longitude. (A) Cross-section of P_1. (B) Cross-section of of $P_{1.5}$. (C) Cross-section of of P_2. (D) Cross-section of of $P_{2.5}$. Magnitude $M_{\mathrm{L}} = 2.5$ represents the reporting threshold level of the Italian Civil Protection. The black contour lines indicate the $P_{2.5} = 0.99$ and $P_{2.5} = 0.999$ level. (E) Cross-section of of $P_{2.9}$. The catalog can be considered complete at the $M_{\mathrm{P}} = 2.9$ level for the entire territory of Italy except for the islands of Sardinia, Pantelleria, and Lampedusa. Contour lines as in frame D. (F) Map of M_{P} at the $P = 0.999$ level. The white contour lines show the $M_{\mathrm{P}} = 2.5$ contour (inner line) and $M_{\mathrm{P}} = 2.9$ contour (outer line).

Figure 5. Maps of scenario computations. The first and second row show $P_{2.9}$ and M_{P} at the $P = 0.999$ level for the computed scenarios, respectively. The white contour lines indicate the detection probabilities of $P_{2.9} = 0.99$ and $P_{2.9} = 0.999$ without any failure, see Figure 2. The red contour lines indicate the same detection probabilities for the scenario computation to visualize the change due to the failure. (first column) Scenario of a failure of the Internet link. (second column) Scenario of a failure of the VPN link. (third column) Scenario of a failure of the satellite link. (forth column) Scenario for the future datacenter with access to satellite-linked stations only.

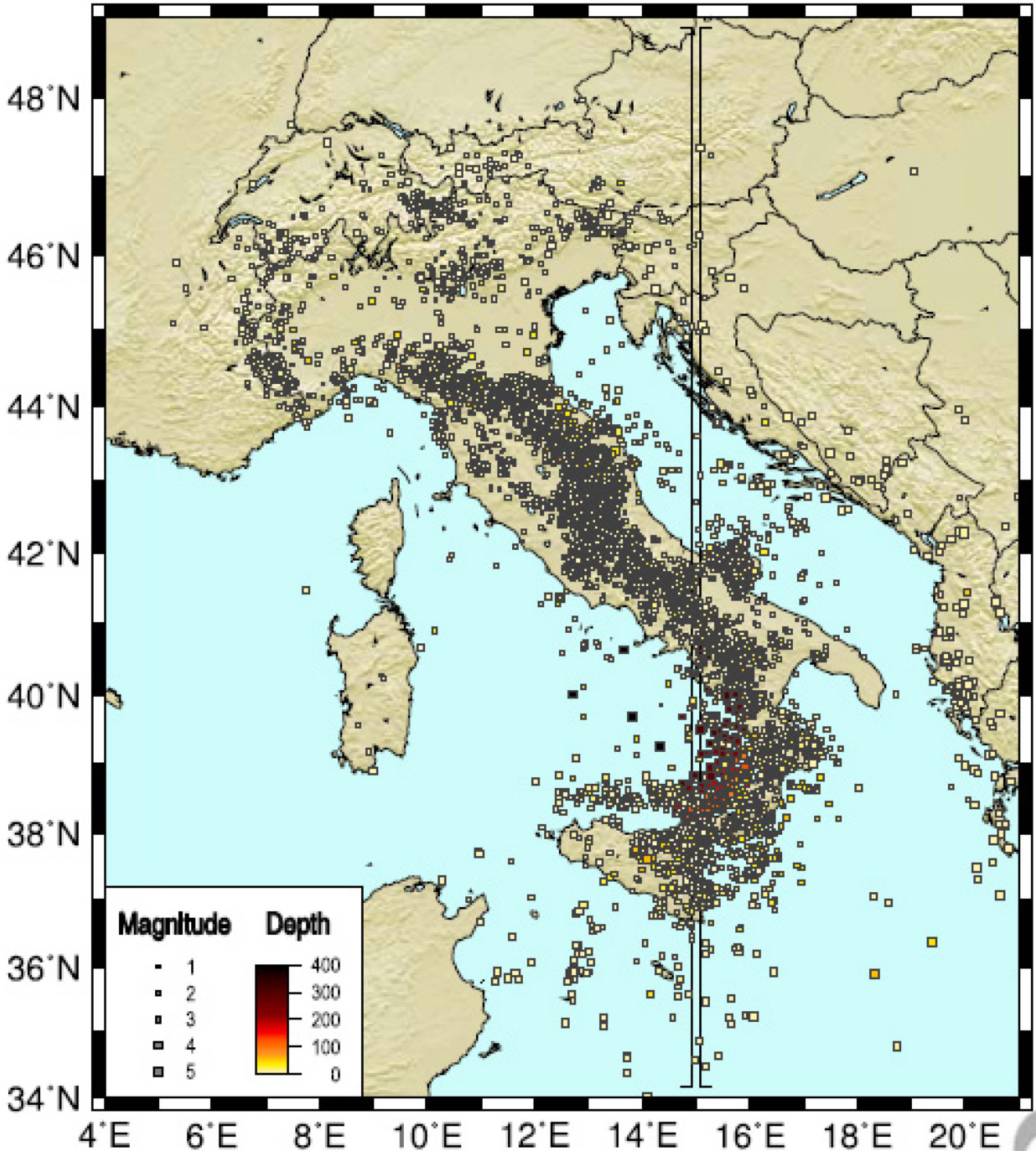
48°N
46°N
44°N
42°N
40°N
38°N
36°N
34°N
4°E
6°E
8°E
10°E
12°E
14°E
16°E
18°E
20°E
Magnitude
1
2
3
4
5
Depth
400
300
200
100
0

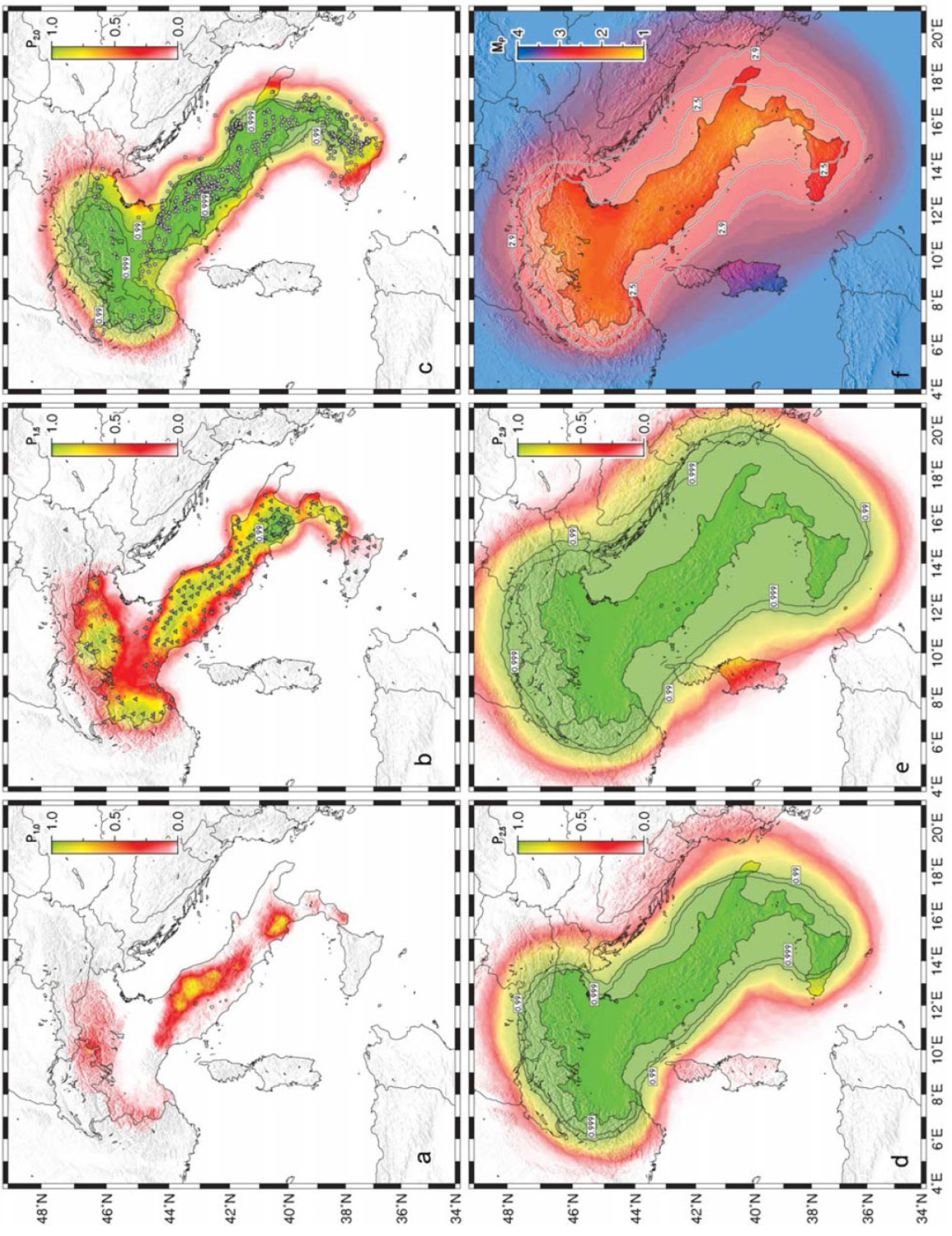
a
b
c
d
e
f
P1.0
P1.5
P2.0
P2.5
P2.9
MP
1.0
0.5
0.0
0.99
0.999
2.5
2.9
48°N
46°N
44°N
42°N
40°N
38°N
36°N
34°N
4°E
6°E
8°E
10°E
12°E
14°E
16°E
18°E
20°E

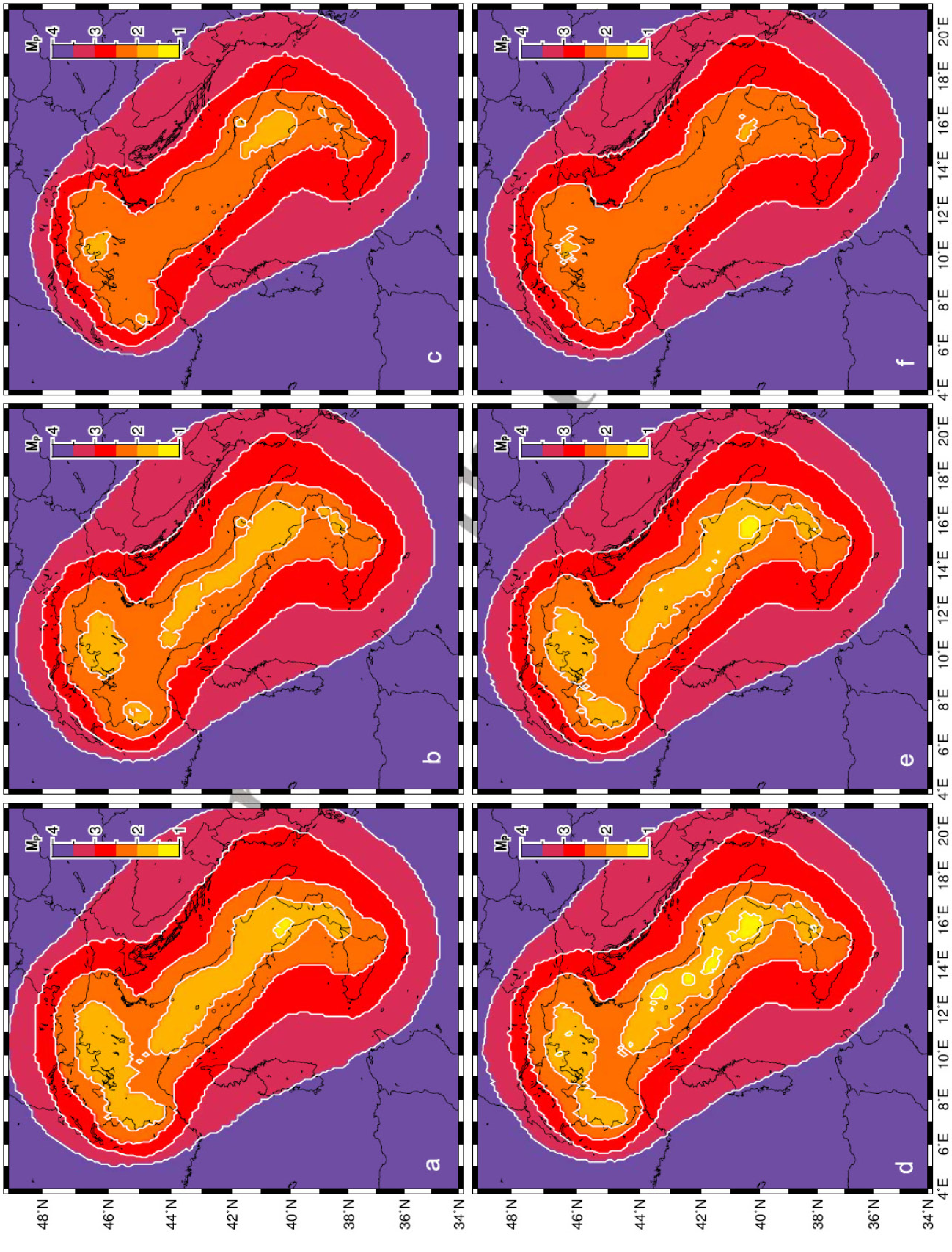
a
b
c
d
e
f
M_P
4
3
2
1
48˚N
46˚N
44˚N
42˚N
40˚N
38˚N
36˚N
34˚N
4˚E
6˚E
8˚E
10˚E
12˚E
14˚E
16˚E
18˚E
20˚E

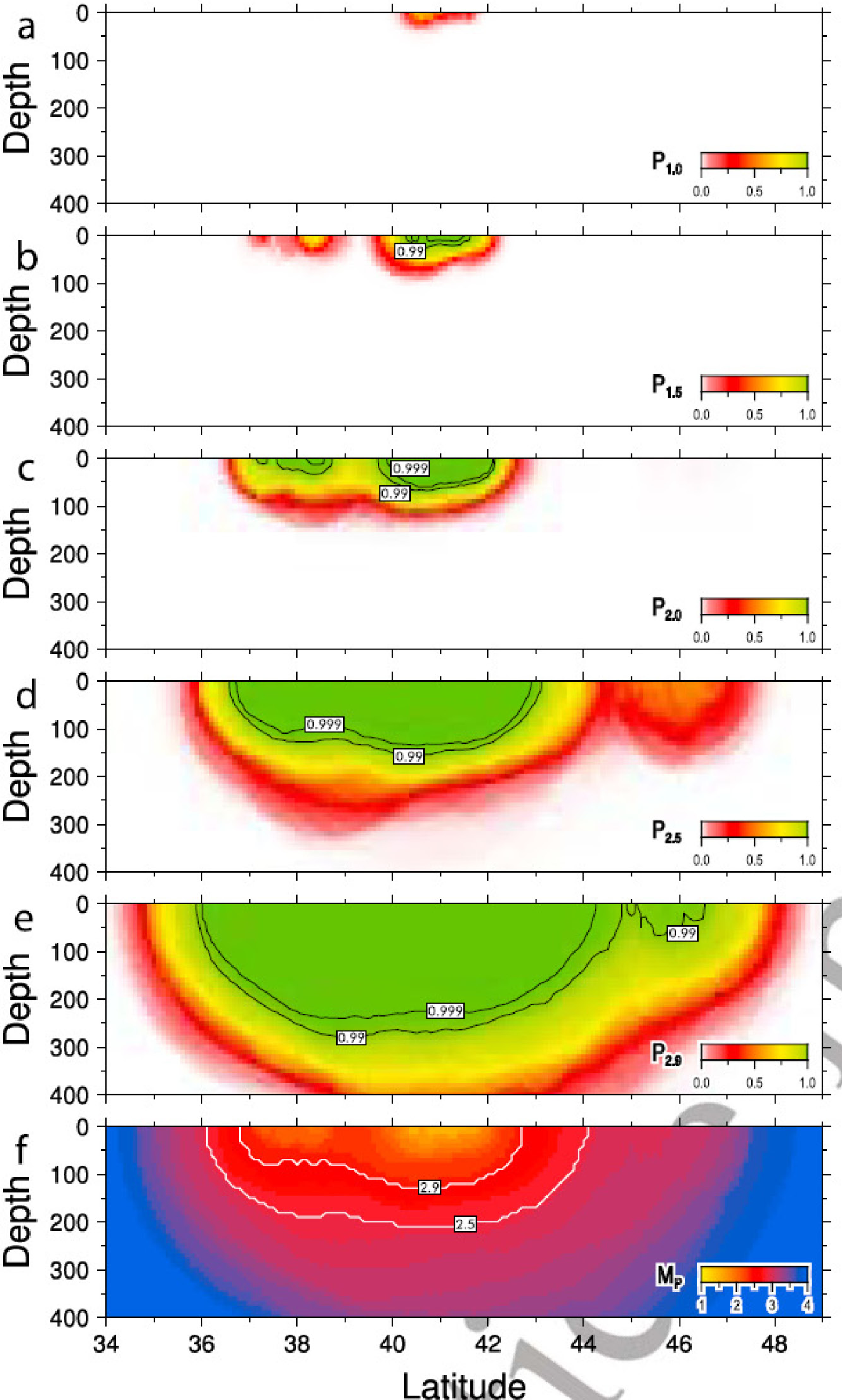
a
b
c
d
e
f
Depth
0
100
200
300
400
0.99
0.999
P1.0
P1.5
P2.0
P2.5
P2.9
MP
2.9
2.5
0.0
0.5
1.0
1
2
3
4
34
36
38
40
42
44
46
48
Latitude

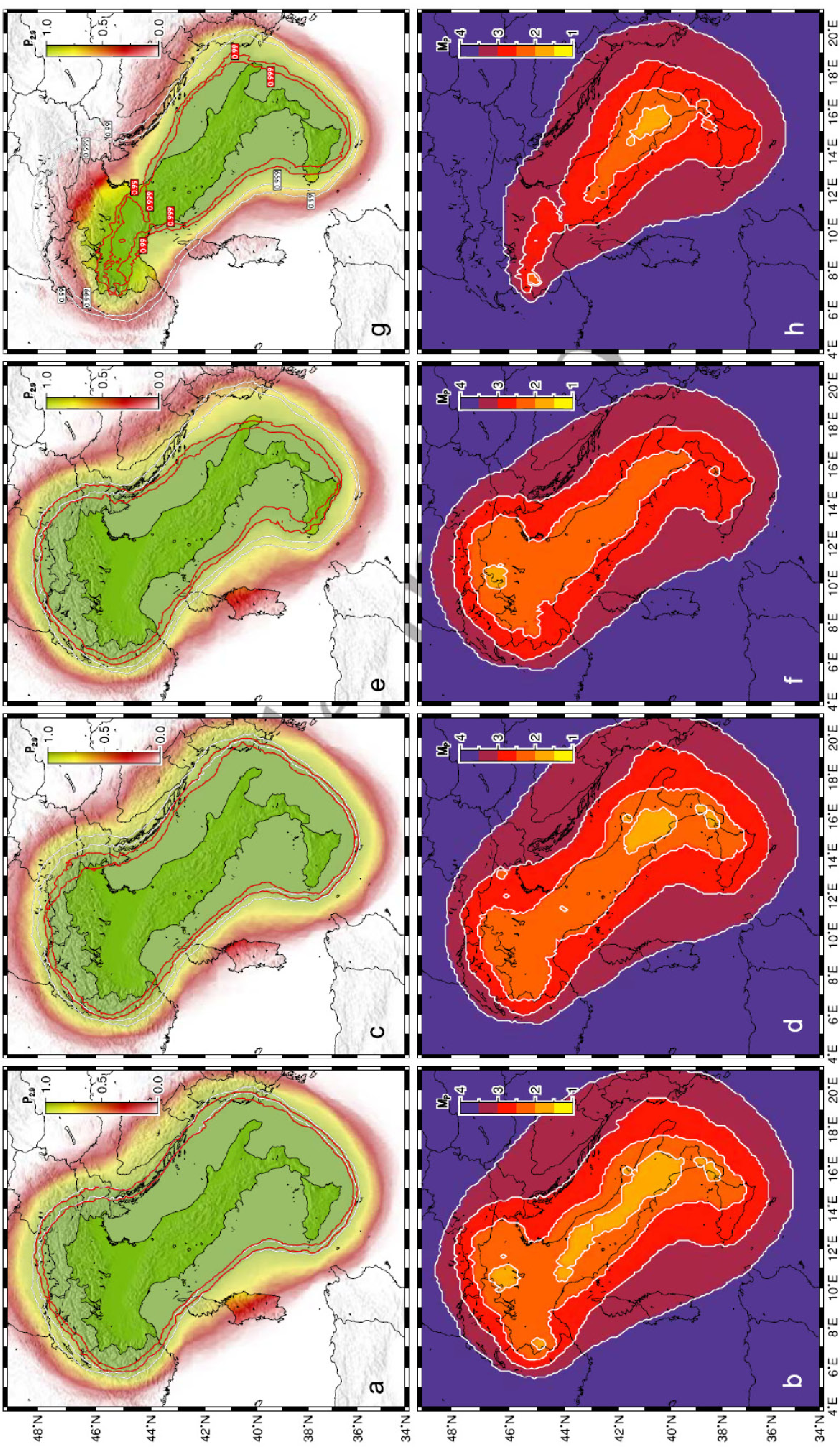
a
b
c
d
e
f
g
h
$P_{2.0}$
1.0
0.5
0.0
M_P
4
3
2
1
0.99
0.999
48°N
46°N
44°N
42°N
40°N
38°N
36°N
34°N
4°E
6°E
8°E
10°E
12°E
14°E
16°E
18°E
20°E